Preprint of Materials Research Letters (2013) doi:10.1080/21663831.2013.856816

Swift Heavy Ion Shape Transformation of Au Nanocrystals Mediated by Molten Material Flow and Recrystallization

A. A. Leino*, O. H. Pakarinen, F. Djurabekova, K. Nordlund

Helsinki Institute of Physics and Department of Physics, University of Helsinki, P.O. Box 43, FI-00014 University of Helsinki, Finland

Emails (respectively): aleksi.leino@helsinki.fi, pakarinenoh@gmail.com, flyura.djurabekova@helsinki.fi, kai.nordlund@helsinki.fi

Phone number: +358 50 3112593

P. Kluth, M. C. Ridgway

Department of Electronic Materials Engineering, Research School of Physical Sciences and Engineering, Australian National University, Canberra, ACT 0200, Australia

Emails: patrick.kluth@anu.edu.au, mcr109@physics.anu.edu.au

Phone numbers (respectively) : +61 2 612 50358, +61 2 612 50519

*Corresponding author.

Swift Heavy Ion Shape Transformation of Au Nanocrystals Mediated by Molten Material Flow and Recrystallization

Swift heavy ion irradiation of amorphous SiO_2 that contains metal nanocrystals can be used to transform the shape of the particles into peculiar asymmetric ones not easily achievable by other means. Using a molecular dynamics simulation framework augmented to include the electronic excitations of the swift heavy ions, we predict that the reshaping of spherical particles into nanorods occurs continuously during consecutive ion impacts by a dynamic crystal-liquid-crystal phase transition of metal particle with the flow of liquid phase into an underdense track core in silica. The simulated nanocrystals are shown to have a saturation width that agrees with experiments.

Keywords: Nanoparticles, Nanocrystals, Elongation, Swift Heavy Ions, Silica

When silica composites that contain spherical metal nanocrystals are subjected to swift ($E_{kin} \geq 1$ MeV / amu) heavy ion (SHI) irradiation, the particles undergo a shape transformation to nanorods or prolate spheroids, so that they elongate in the direction parallel to the ion beam.[1–14] This effect is analogous to the well established possibility to use multiwall carbon nanotubes inside an electron microscope as pressure vessels to modify and study the properties of metal nanocrystals.[15, 16] The swift ion processing has, however, the major advantage that the end result is stable over macroscopic timescales when taken out of the experimental processing chamber. Therefore, in addition to being a directly observable nanoscale test system for understanding the fundamentals of ion-solid interactions, the phenomenon has application potential. By controlling the dimensions of the crystal by swift heavy ion (SHI) irradiation, control over surface plasmon resonance is gained,[17, 18] which is desirable in the fabrication

of plasmonic devices.[19] The method has the advantage of producing large arrays of equally aligned nanocrystals, which is difficult to achieve otherwise.

In this letter, we examine the nanocluster shape transformation mechanisms using classical Molecular Dynamics (MD) simulations, extended with the inelastic thermal spike model (i-TS),[20] and experiments. The experiments show a major elongation effect similar to that reported previously by other groups.[1–14] The MD simulations with the i-TS energy deposition reproduce the experimentally observed progressive elongation. The minor axis of the elongated particle is shown to saturate at a width correlated with the width of the ion track in silica,[4] in excellent agreement with experiments. The results show that the elongation is caused by the thermal expansion associated with heating and melting of *crystalline* metal, which causes it to flow within the track core in silica.

Although technologically promising, the elongation mechanism of nanocrystals by SHIs has not yet been identified. In the energy range of SHI's, the primary interactions between the ion and the irradiated material are dominated by collisions with electrons, and the kinetic energy of the ion is first consumed in the excitation of the electronic subsystem.[21] D'Orléans et al. [1] calculated that there is a large overpressure in the crystal after impact, which is released by flow of molten matter to the track in silica. However, it was not clear why the nanocrystals resist deformation when embedded in a crystalline matrix.[22] Another proposed reason is the so called "ion-hammering" effect,[23] which is characteristic for an amorphous matrix and leads to an in-plane stress, which might deform the metal particle once melted. Klaumünzer [2] considered both ion hammering and melting, concluding that ion hammering could not be the cause of deformation, whereas a rough estimate showed that, at least within an order of magnitude, the high pressure in molten metal could explain the elongation. Dawi et al. [8] found the effect to be sensitive, under certain conditions, to the initial concentration of the nanoparticles. However, such behavior could be associated with Ostwald

ripening, which was avoided in [7] by forcing a large distance between individual Au nanoparticles. Results in this study confirmed that elongation can proceed through individual processes. Amekura et al. also observed that a small change in the shape of the nanocrystals was induced by single impacts.[12]

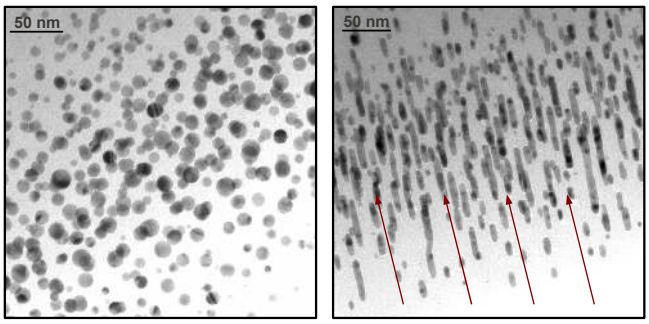

Figure 1: Modification of the shapes of Au nanocrystals embedded in silica into strongly elongated nonequilibrium shapes. Left: Cross-sectional transmission electron microscopy (XTEM) image of the initial shape of spherical nanocrystals. Right: XTEM image of nanocrystals with the same initial radius after swift heavy ion irradiation (direction indicated by arrows) with 54 MeV Au ions with a fluence of 2×10^{14} ions/cm^2. Thanks to the surrounding inert silica matrix, the final shape is very stable at ambient conditions.

Au nanocrystals were formed in thermally-grown SiO_2 by ion implantation and annealing. Samples were then irradiated with 185 MeV Au^{+13} ions at normal incidence and room temperature. Transmission electron microscope in a cross section geometry was utilised to determine the dimensions of the elongated nanocrystals (see Fig. 1), measuring 300 crystals for reasonable statistics. Additional details on the experimental procedure is given in [9, 11].

The computer simulations were performed by using a multiscale model implemented in the classical MD code PARCAS [24] to simulate the elongation. Classical MD [25] can be used to study the transport of the atoms from given initial conditions, but it does not explicitly describe the electronic subsystem or its coupling to the atomic subsystem (see Supplementary Material for the advantages and limitations). The initial nanocrystal was generated following a procedure described by Djurabekova,[26] i.e cutting a sphere out of fcc Au, compressing it by 2% to avoid unrealistically low inter-

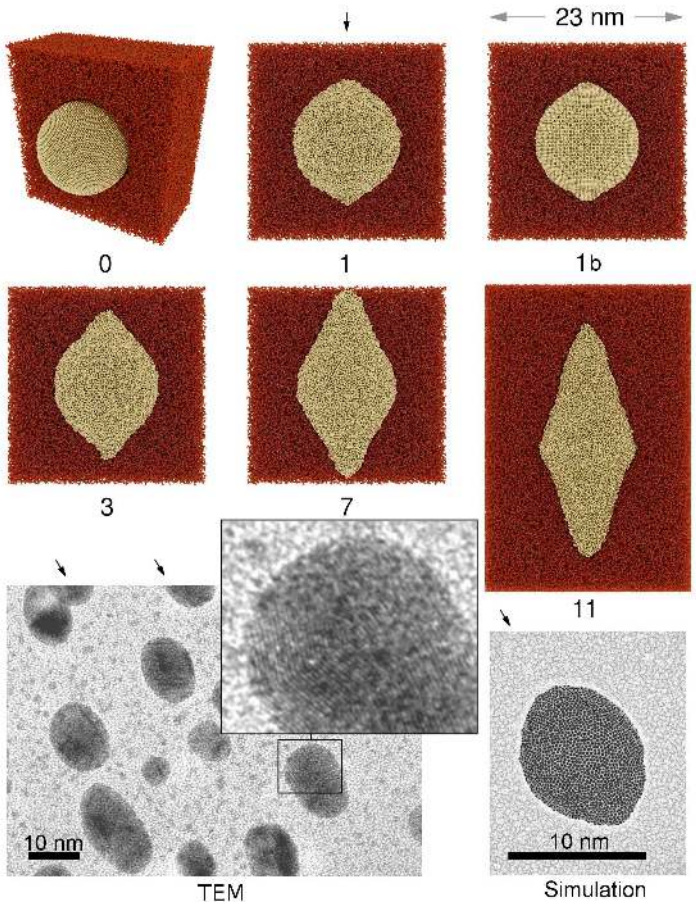

Figure 2: Elongation of Au nanocrystals in silica in MD simulations (colored images). Each image shows a cross section of the simulation cell 50 ps after the ion impacts. The top row shows the initial cluster (0) and the shape after the recrystallization procedure (1b). Shown below each image is the total number of impacts. The energy deposited to the cell corresponds to an ion intersecting through the middle of the crystal, as indicated by the black arrow. The lower left image shows an experimental TEM image at an intermediate dose, and the lower right image shows the simulated shape after three non-overlapping impacts. The inset in the lower left image shows a zoom of one of the crystals, showing the crystalline lattice planes.

atomic separations in the initial configuration, and inserting this sphere into a bigger void than the uncompressed sphere in silica (see Fig. 2, case (0)). The resulting cell was then pressure and temperature relaxed for 50 ps to cancel the compression of the cluster (see above) and to obtain a stable, well-relaxed metal nanocrystal embedded in silica.

For silica interactions (Si-O, Si-Si, O-O), the Watanabe-Samela interatomic poten-

tial was used,[27, 28] and for gold (Au-Au), the EAM potential.[29] The gold potential reproduces the parameters relevant to thermal expansion well (See Supplementary Material for details). Gold-silica interactions were implemented using pair potentials as explained in the Supplementary Material and previous work.[30]

The effect of the swift heavy ion was implemented by assigning randomly distributed velocities obtained from the i-TS to the atoms at the beginning of the simulation. The i-TS model is a phenomenological model which utilises heat equations to describe the temperatures of the atomic and electronic subsystems as a function of time, and has yielded a good agreement with experiments over a wide range of irradiation conditions and materials.[20] The same combined simulation approach was used to study the fine structure of ion tracks in pure silica, revealing a low density core – high density shell structure in agreement with experiments.[4]

For silica, the distribution of kinetic energy *vs.* radial distance from the ion path was extracted from the i-TS model for a 164 MeV Au ion at 100 fs from impact by a equilibrium temperature to kinetic energy conversion (some details of the i-TS calculation are given in the Supplementary Material). Even though this approach does not include further heat transfer between atomic and electronic subsystems, it is justified within the i-TS model since most of the heat transfer from the electrons to the lattice occurs within this time. Since the Watanabe-Samela potential overestimated the glass transition temperature approximately a factor of 2 (we calculated 3500 $\pm$ 500 K, whereas the experimental [31] is 1995 K), the energy deposition from the i-TS model was scaled up by the same factor to match the homologous temperatures. This approach yielded track features in pure silica that matched those of experimentally measured tracks.[4] Motivated by the very rapid electronic heat conduction in Au, a constant energy of 0.5 eV/atom was deposited to Au nanocluster atoms at the same time as the deposition to silica atoms. Tests of other energy deposition schemes showed that the elongation mechanism is not sensitive to the exact energy deposition to Au, as long as sufficient

energy is provided to melt the cluster (see Supplementary Material for details).

To mimic heat conduction to the bulk and to dampen pressure waves that travel through the periodic boundary, the Berendsen thermostat [32] was applied at the borders of the cubical simulation cell. The width of the boundary cooling region is about 10% of the total cell width, which was 23 nm. We extended the cell size to 33 nm in the ion beam direction to accommodate nanocrystals whose major axis had grown close to the original cell height. After the swift heavy ion energy deposition was performed, the evolution of the system was followed for 100 ps. During the last 50 ps, no significant changes in the cluster shape were found to occur.

In a single ion simulation, we observe that the gold nanocrystal first melts by the swift heavy ion energy deposition during the first few ps after the ion impact. During the same time scale, an underdense silica track core forms as described previously.[9] The crucial stage for elongation is about 5-20 ps after the impact when the molten, pressurized nanocluster expands (see Figs. 3, 4 and movie in the Supplementary Material) by a longitudinal flow of Au atoms into the underdense core of the silica track. After about 20 ps, silica cools down below the glass transition temperature and the evolution of the nanocluster shape stops.

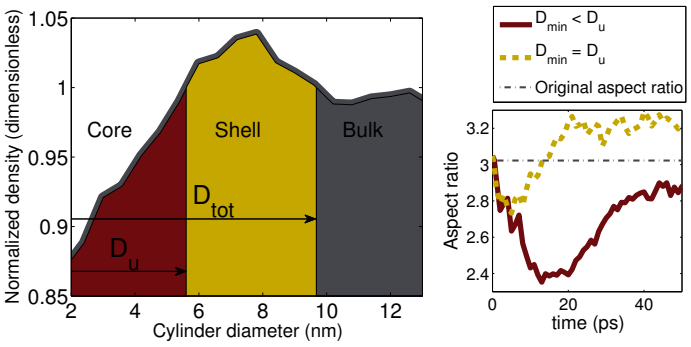

Figure 3: The final core-shell structure in the density profile of the silica track for the simulated 164 MeV Au ion and the evolution of the aspect ratio of nanocrystals whose diameter (D_{minor}) is smaller than the diameter of the underdense core (D_u) or equal to it.

The atomic structure in the cluster remained amorphous within the computed sim-

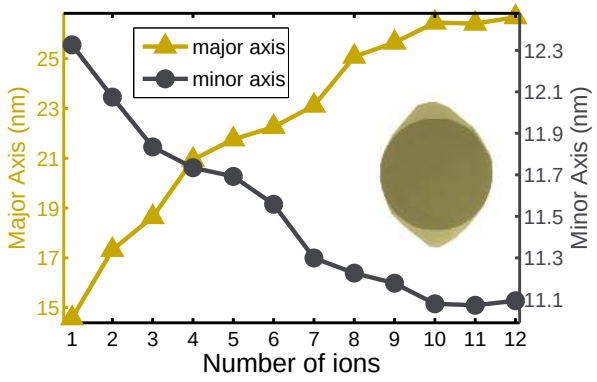

Figure 4: Evolution of the dimensions of r = 6 nm cluster as a function of ion impacts. Shown also the shape of the cluster before and after first impact. The overlap of these regions appear dark. Note that contrary to our previous study, the current study reproduces the loss of width of the cluster (see figures 3 and 4 in [30]). This demonstrates the importance of the recrystallization.

ulation time (100 ps). Close inspection of the experimental images of elongated clusters (see the experimental image inset in Fig. 2) shows that they are crystalline or polycrystalline, in agreement with previous work.[33] Test simulations on longer (ns) timescales showed that the cluster evolved towards a polycrystalline state, in agreement with the experiments, but simulation of full recrystallization was not practical due to the limited time scale of MD simulations.[25] From the experimental ion fluxes and known nanocrystal diameters [9, 11] it is clear that the typical time scale between ion impacts on an individual nanocrystal is of the order of seconds. Therefore it is straightforward to assume that the simulated nanoclusters would naturally crystallize before the next ion impact. Hence we introduce a simple recrystallization scheme in which we construct a new simulation cell as the initial cell, but instead of using a crystalline sphere as the nanocrystal, the shape of the cluster 50 ps after every impact is used (see Fig. 2). The atom count of the particle is preserved within ± 15 atoms.

On subsequent impacts, using the recrystallization procedure, the elongation proceeds gradually from a sphere to a rod-like shape (see Fig. 2, Fig. 4 and the movie in the Supplementary Material.) Without the inclusion of the recrystallization, the shape

transformation does not continue after the first impact.[30] MD calculations using the EAM potential showed that an amorphous cluster has about 4% higher volume than a crystalline cluster with equal atom count (30 000) at 300K. The gain in volume lowers the thermal expansion pressure of the cluster as the crystal melts during the next ion impact. We found this pressure to be essential for the shape transformation. Therefore if the cluster is left amorphous, the elongation observed in the experiment can never be achieved. On the contrary, with the recrystallization step we obtain a continued elongation (Fig. 4) which agrees quantitatively with experiments (Fig. 5).

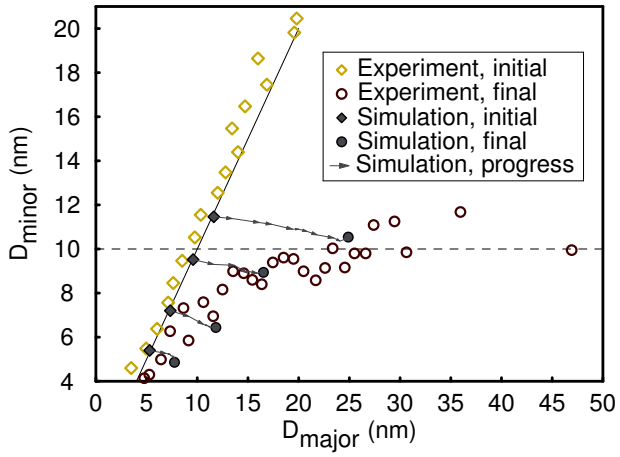

Figure 5: Plot of the dimensions of the nanocrystals before and after irradiation. Blank diamonds and circles indicate the dimensions of the initial experimental nanocrystal population and after a fluence of 2×10^{14} ions per cm^2, respectively. Filled diamonds and circles show the evolution of the simulated nanocrystals. Each arrow represents one impact. Dashed line shows the approximate saturation width of the largest nanocrystals in the experiments.

The simulation cells are initially stress-free (except for the transient thermal stresses introduced by the ion itself). Hence the current simulations show that the first stages of the elongation can be explained by thermal expansion and flow of matter from the nanocluster into the track core, and is not a consequence of an ion-hammering effect or any diffusion-like processes.

Some difference in the final elongated shapes obtained experimentally and in the simulations is evident. In the current simulations all the SHI impacts were simulated

through the centre of the nanocrystal to keep the focus on the main underlying mechanism for its elongation. At the same time the experimental impacts can not be expected to act likewise. Analysis of the experimental TEM image of the elongated nanocrystals (see TEM image in Fig. 2) reveals shape asymmetry for some nanocrystals, which was also observed in our earlier simulations of random-position SHI impacts on Au nanoclusters.[30] Also, clusters in these simulations appeared more round at the bottom and at the top, as seen in the simulated image next to the TEM image in Fig. 2. In some experimental works, the shapes of elongated nanocrystals similar to the currently simulated "lemon-like" ones were also observed (e.g. in [14]).

We next turn to the question of why the elongation experiments show a critical width of the particle, below which no or little elongation occurs.[9, 17] Plotting the experimental nanocrystal population on a graph according to their minor and major diameters (D_{minor}, D_{major}) before and after irradiation shows that the largest crystals have a width comparable to the track size in silica and that the small nanocrystals are not elongated as efficiently (see Fig. 5). After a dose of 2×10^{14} ions per cm^2, further irradiation induces no significant changes in the curve. This enables a comparison between the simulations and experiment. We prepared four simulation cells with spherical nanocrystals using different diameters and performed ion impact simulations as described above until no significant changes were observed in the dimensions of the nanocrystals. We then placed the simulated evolution of the maximal width and height of the crystals on the (D_{minor}, D_{major}) graph. The simulated final distribution is similar to the experimental one, as shown by the circles in Fig. 5.

Since the simulations of multiple impacts on the same nanocrystal consume very large amounts of CPU time, we also constructed a test system designed to study specifically the saturation, i.e. a rod-like nanocrystal with $D_{minor} = 6$ nm, $D_{major} = 12$ nm. Two different energy deposition profiles were then used in an impact simulation. The first produces a track where the underdense core is larger than the minor axis of

the cluster, and the second produces one which is equal to the minor axis.

These simulations enable us to identify the basic *reason behind saturation width dependence on the track size in silica* [10]: when the underdense track is larger than the minor axis of the nanocluster, it expands in all three directions. In the opposite case, the nanocluster is unable to expand in the directions perpendicular to the ion as efficiently as in the parallel direction. Therefore the cluster is growing in aspect ratio. Due to the high temperatures in silica in the vicinity of the ion trail, the pressure exerted from silica to the cluster prevents the growth for a short time before the track core cools down, as seen from the evolution of the aspect ratios in Fig. 3.

The saturation width of the largest nanocrystals matches quite well with the track radius, which includes both the underdense core and the overdense shell of the ion track (see Fig. 3 and Fig. 5), both in the simulations and experiments. Similar behaviour was experimentally observed by Ridgway et al. [11] for several other metal species, but some materials appear to saturate at a lower width (e.g. platinum).

In single impact simulations, the rod-like crystals whose widths are smaller than the underdense track core (see Fig. 3) are not growing in aspect ratio whereas bigger ones are. It might be therefore expected that the saturation width is equal to the width of the underdense track. We note that the increment in the major axis dimension has to be sufficiently large for the nanocrystal to subsequently elongate, since some of the increment is lost during the recrystallization to minimize surface energy. When the minor axis of the crystal is equal to the underdense core, growth in aspect ratio occurs initially, but most of it is lost during the recrystallization. The major axis growth is sufficient for elongation only when the minor axis is clearly larger than underdense core. Hence the saturation width that is obtained in Fig. 5 is larger than the diameter of the underdense core.

In conclusion, we have performed MD simulations in conjunction with the inelastic thermal spike model that reproduce the experimentally observed elongation of Au

nanocrystals under SHI irradiation. In the simulations, the elongation is caused by an anisotropic thermal expansion of the molten nanocluster within the underdense track core in silica. Nanocrystals whose minor axis is smaller than the diameter of the underdense track expand more isotropically and are not elongated, which leads to a saturation of the width of the crystals. The saturation width was also observed experimentally. The results imply that both formation of an underdense track in silica and shape-conserving crystallization of the molten cluster between ion impacts are necessary prerequisites for elongation of metallic nanocrystals by swift heavy ion impacts.

Aknowledgements

This project was funded by the Academy of Finland and the National Doctoral Programme in Nanoscience (NGS) of Finland. The authors thank Marcel Toulemonde for providing the energy deposition profile for SiO_2 and CSC - IT Center for Science Ltd (Finland) for grants of computation time. P.K. and M.C.R. thank the Australian Research Council for support.

References

[1] D'Orléans C, Stoquert JP, Estournes C, Cerruti C, Grob JJ, Guille JL, Haas F, Muller D, Richard-Plouet M. Anisotropy of Co nanoparticles induced by swift heavy ions. Phys Rev B. 2003;67:220101.

[2] Klaumünzer S. Modification of nanostructures by high-energy ion beams. Nucl Instr Meth Phys Res B. 2006;244(1):1–7.

[3] Rizza G, Dunlop A, Dezellus A. Behavior of metallic nanoparticles in Al matrix under high electronic energy deposition. Nucl Instr Meth Phys Res B. 2007;256(1):219–223.

[4] Kluth P, Schnohr CS, Pakarinen OH, Djurabekova F, Sprouster DJ, Giulian R, Ridgway MC, Byrne AP, Trautmann C, Cookson DJ, Nordlund K, Toulemonde M. Fine structure in swift heavy ion tracks in amorphous SiO_2. Phys Rev Lett. 2008;101:175503.

[5] Reyes-Esqueda JA, Rodriguez-Iglesias V, Silva-Pereyra HG, Torres-Torres C, Santiago-Ramirez AL, Cheang-Wong JC, Crespo-Sosa A, Rodriguez-Fernandez L, Lopez-Suarez A, Oliver A. Anisotropic linear and nonlinear optical properties from anisotropy-controlled metallic nanocomposites. Optics Express. 2009;17(5):12849–12868.

[6] Awazu K, Wang X, Fujimaki M, Tominaga J, Aiba H, Ohki Y, Komatsubara T. Elongation of gold nanoparticles in silica glass by irradiation with swift heavy ions. Phys Rev B. 2008;78:054102.

[7] Awazu K, Wang X, Fujimaki M, Komatsubara T, Watanabe J, Matsumoto Y, Warisawa S, Ishihara S. The fabrication of aligned pairs of gold nanorods in SiO_2 films by ion irradiation. Nanotechnology. 2009;20:325303.

[8] Dawi EA, Rizza G, Mink MP, Vredenberg AM, Habraken FHPM. Ion beam shaping of Au nanoparticles in silica: Particle size and concentration dependence. J Appl Phys. 2009;105:074305.

[9] Kluth P, Giulian R, Sprouster DJ, Schnohr CS, Byrne AP, Cookson DJ, Ridgway MC. Energy dependent saturation width of swift heavy ion shaped embedded Au nanoparticles. Appl Phys Lett. 2009;94(11):113107.

[10] Avasthi DK, Mishra YK, Singh F, Stoquert JP. Ion tracks in silica for engineering the embedded nanoparticles. Nucl Instr Meth Phys Res B. 2010;268:3027–3034.

[11] Ridgway MC, Giulian R, Sprouster DJ, Kluth P, Araujo LL, Llewellyn DJ, Byrne AP, Kremer F, Fichtner PFP, Rizza G, Amekura H, Toulemonde M. Role of Thermodynamics in the Shape Transformation of Embedded Metal Nanoparticles Induced by Swift Heavy-Ion Irradiation. Phys Rev Lett. 2011;106(9):095505.

[12] Amekura H, Ishikawa N, Okubo N, Ridgway MC, Giulian R, Mitsuishi K, Nakayama Y, Buchal C, Mantl S, Kishimoto N. Zn nanoparticles irradiated with swift heavy ions at low fluences: Optically-detected shape elongation induced by nonoverlapping ion tracks. Phys Rev B. 2011;83(20):205401.

[13] Dufour C, Khomenkov V, Rizza G, Toulemonde M. Ion-matter interaction: the three-dimensional version of the thermal spike model. Application to nanoparticle irradiation with swift heavy ions. J Phys D Appl Phys; 45:065302.

[14] Rizza G, Coulon PE, Khomenkov V, Dufour C, Monnet I, Toulemonde M, Perruchas S, Gacoin T, Mailly D, Lafosse X, Ulysse C, Dawi EA. Rational description of the ion-beam shaping mechanism. Phys Rev B. 2012;86:035450.

[15] Sun L, Banhart F, Krasheninnikov AV, Rodriguez-Manzo JA, Terrones M, Ajayan PM. Carbon nanotubes as High-Pressure Cylinders and Nanoextruders. Science. 2006;312:1199.

[16] Sun L, Krasheninnikov AV, Ahlgren T, Nordlund K, Banhart F. Plastic deformation of single nanometer-sized crystals. Phys Rev Lett. 2008;101:156101.

[17] Mishra YK, Singh F, Avasti DK. Synthesis of elongated Au nanoparticles in silica matrix by ion irradiation. Appl Phys Lett. 2007;91:063103.

[18] Link S, El-Sayed MA. Spectral Properties and Relaxation Dynamics of Surface Plasmon Electronic Oscillations in Gold and Silver Nanodots and Nanorods. J Phys Chem B. 1999;103(40):8410–8426.

[19] Barnes WL, Dereux A, Ebbesen TW. Surface plasmon subwavelength optics. Nature. 2003;424:824–830.

[20] Toulemonde M, Assmann W, Dufour C, Meftah A, Studer F, Trautmann C. Experimental phenomena and thermal spike model description of ion tracks in amorphisable inorganic insulators. Mat Fys Medd Kong Dan Vid Selsk. 2006;52:263.

[21] Ziegler JF, Biersack JP, Littmark U. The Stopping and Range of Ions in Matter. New York: Pergamon; 1985.

[22] Kerboua CH, Chicoine M, Roorda S. Gold nanoparticles resist deformation by swift heavy ion irradiation when embedded in a crystalline matrix. Nucl Instr Meth Phys Res B. 2011;269(18):2006 –2010.

[23] Benyagoub A, Löffler S, Rammensee M, Klaumünzer S, Saemann-Ischenko G. Plastic deformation in SiO_2 induced by heavy-ion irradiation. Nucl Instr Meth Phys Res B. 1992;65(14):228 –231.

[24] Nordlund K. PARCAS computer code. The main principles of the molecular dynamics algorithms are presented in [34, 35]. The adaptive time step is the same as in [36]. 2006.

[25] Allen MP, Tildesley DJ. Computer Simulation of Liquids. Oxford, England: Oxford University Press; 1989.

[26] Djurabekova F, Nordlund K. Atomistic simulation of the interface structure of Si nanocrystals embedded into amorphous silica. Phys Rev B. 2008;77:115325.

[27] Watanabe T, Yamasaki D, Tatsumura K, Ohdomari I. X. Appl Surf Sci. 2004;234:207.

[28] Samela J, Nordlund K, Popok VN, Campbell EEB. Origin of complex impact craters on native oxide coated silicon surfaces. Phys Rev B. 2008;77:075309.

[29] Foiles SM, Baskes MI, Daw MS. Embedded-atom-method functions for the fcc metals Cu, Ag, Au, Ni, Pd, Pt, and their alloys. Phys Rev B. 1986;33(12):7983.

[30] Leino AA, Pakarinen OH, Djurabekova F, Nordlund K. A study on the elongation of embedded Au nanoclusters in SiO_2 by swift heavy ion irradiation using MD simulations. Nucl Instr Meth Phys Res B. 2012;282:76–80.

[31] Haynes WM. CRC Handbook of Chemistry and Physics, 93rd Edition (Internet Version 2013). Boca Raton, FL, USA: CRC Press/Taylor and Francis; 2012-2013.

[32] Berendsen HJC, Postma JPM, Gunsteren WF, DiNola A, Haak JR. Molecular dynamics with coupling to external bath. J Chem Phys. 1984;81(8):3684.

[33] Silva-Pereyra H, Arenas-Alatorre J, Rodriguez-Fernandez L, Crespo-Sosa A, Cheang-Wong J, Reyes-Esqueda J, Oliver A. High stability of the crystalline configuration of Au nanoparticles embedded in silica under ion and electron irradiation. J Nanopart Res. 2010;12:1787–1795.

[34] Nordlund K, Ghaly M, Averback RS, Caturla M, Diaz de la Rubia T, Tarus J. Defect production in collision cascades in elemental semiconductors and FCC metals. Phys Rev B. 1998;57(13):7556–7570.

[35] Ghaly M, Nordlund K, Averback RS. Molecular dynamics investigations of surface damage produced by keV self-bombardment of solids. Phil Mag A. 1999;79(4):795.

[36] Nordlund K. Molecular dynamics simulation of ion ranges in the 1 – 100 keV energy range. Comput Mater Sci. 1995;3:448.

Swift Heavy Ion Shape Transformation of Au Nanocrystals Mediated by Molten Material Flow and Recrystallization

Supplementary Material

A.1. Animation

The supplementary information includes the animation,[1, 2] which shows first the MD simulation of the elongation of a d=12nm Au nanocluster embedded in silica by the first impacting swift heavy ion, then the end results of subsequent impacts.

The small red spheres show the positions of Si and the small orange-brown spheres of O atoms. The large yellow spheres show the positions of Au atoms. The ions (which are not explicitly shown) come from the top and travel straight downwards. Their energy deposition to the SiO_2 atoms is modeled with the inelastic thermal spike model as described in the main text.

A.2. Details of the energy deposition

The energy deposition for silica calculated using the i-TS model for 164 MeV Au ion is given in figure 1. This profile is extracted by converting the lattice temperatures to kinetic energy when the temperature has reached maximum, i.e. after about 100 fs from the beginning of the calculation. The same profile was used for the calculations performed in Ref. [3] and it produces the track radius in agreement with experiments.

The conventional i-TS model cannot describe the electronic Schottky barrier of 4 eV [4] at the gold-silica interface. This will likely have an effect on the electronic heat transport, and thus the exact energies obtained by the gold atoms by 164 MeV Au ion impact remains unknown. Because of the low electron-phonon coupling, we expect a uniform heat distribution, i.e. no spatial dependence of the electronic energy deposition profile for Au atoms. The energy deposition to Au atoms was chosen to be 0.5 eV / atom, which is enough to melt the cluster. This heats the particle initially to 2000 K, which is in agreement with the peak temperature of a similar particle in the calculations of Awazu et al.[5] The magnitude of this value does not affect our conclusions, since the elongation occurs qualitatively similar on a wide range of Au deposition energies,[6] provided that the cluster melts at least partially. The energy deposited to the gold cluster determines the rate of major axis growth during the first 15 ps (for the simulated 164 MeV Au ion) from impact. After this time, the track in silica has frozen whereas the gold particle has not and the elongation stops, without noticeable dependence on energy deposition to the particle.

Furthermore, the i-TS model predicts that gold heats up much slower than silica due to its low electron-phonon coupling. Therefore the instantaneous energy deposition is not necessarily valid. However, qualitative results from our simulations are insensitive

to the applied energy deposition model. To examine whether this affects the elongation, we perfomed a simulation in which the cluster was heated from the initial 300 K to 2000 K in 10 ps (again following Awazu *et al.* [5]) time with the Berendsen thermostat, while applying the instantaneous i-TS deposition profile to silica. We found that this did not have effect on the qualitative features of the shape transformation. Hence we decided to use the simple, instantaneous energy deposition for both gold and silica for the results reported here.

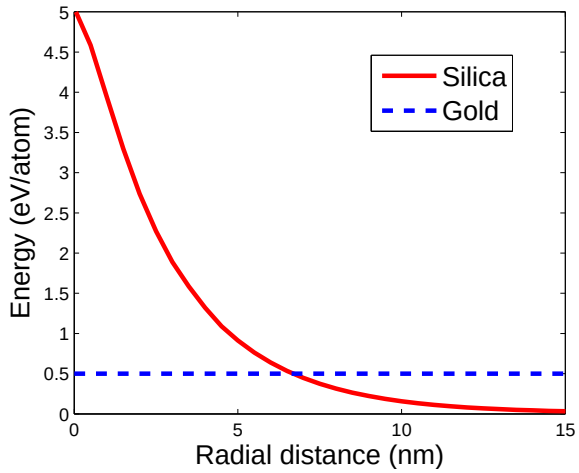

Figure 1: The energy deposition profiles for silica and gold.

A.3. Pair potentials used for Au-Si Au-O interactions

Our previous studies of the same system with different gold-silica interface potentials showed that there is a threshold energy of interaction between gold and silica (about 0.2 eV per atom pair). Above this threshold the gold atoms escaped into the silica matrix on any impact and hence no shape transformation dynamics can be observed. The threshold value was found by using Morse potentials fitted to the DFT Au-Si, Au-O dimer calculations [6] with subsequent rescaling of potential wells. Using weak attractive wells, which correspond to reports of a very weak attraction between Au and Si/O at large distances,[7–9] we did observe an elongation similar to that reported in the main text.

A negligible chemical interaction with silica surface (except with certain defect sites) was confirmed both experimentally and theoretically. Moreover, it was found that the penetration barrier of gold atoms through silica rings is high.[7–9] Therefore the use of attractive potentials that have a strong interaction energy and thus cause unavoidable dissolution of the cluster is not physically well founded.

To capture the chemical inertness and the high penetration barrier of the surface, the Au-O and Au-Si interactions were modeled with ZBL [10] pair potentials. This potential

Table 1: Parameters of thermal expansion.

Parameter	Experimental [11]	Potential
Volumetric thermal expansion coefficient[1] at 25°C	42.6 $\frac{10^6}{\mathrm{K}}$	38.9 $\frac{10^6}{\mathrm{K}}$
Melting point	1 337.33 K	(1110 ± 20) K
Density at 25°C	$19.3 \frac{\mathrm{g}}{\mathrm{cm}^3}$	19.1 $\frac{\mathrm{g}}{\mathrm{cm}^3}$
Density at 1337.33 K (molten)	$17.31 \frac{\mathrm{g}}{\mathrm{cm}^3}$	17.5 $\frac{\mathrm{g}}{\mathrm{cm}^3}$
Derivative of the density above the melting point	$0.001343 \frac{\mathrm{g}}{\mathrm{cm}^3\mathrm{K}}$	$0.0013 \frac{\mathrm{g}}{\mathrm{cm}^3\mathrm{K}}$

prevents the gold atoms from dissolving into silica through the silica rings during the impact simulation. In contrast to strongly attractive potentials, it also enables the segregation of Au atoms on annealing, which is a prerequisite for the formation of the nanocrystals.

The choice of the potential results in additional pressure accumulated on the cluster after the impact. This may affect only the rate of elongation, for this pressure alone will not be sufficient to cause a flow of gold atoms into the open track and thus cannot be crucial for the mechanism of elongation. Because of this and the uncertainty that stems from the energy deposition model, we currently do not relate the experimental rate of elongation to the simulated one.

A.4. Thermal expansion reproduced by the gold potential

Parameters related to thermal expansion are given in table 1. It is important for the proposed elongation mechanism that they are reproduced well. All values are in reasonable agreement with experiments, which means both the volume expansion upon melting and the thermal expansion in solid and molten state are reproduced well.

A.5. Advantages and limitations of the calculation techniques

The inelastic thermal spike model (i-TS) has succesfully explained track formation silicon dioxide.[12] It can give quantitative predictions in agreement with experiments, which remains difficult for many of the other models suggested to be responsible for

track formation.[13]

The model consists of two coupled heat equations for the electronic subsystem and for the atomic (sometimes also referred to as ionic) subsystem. The energy is first inserted to the electronic subsystem using a formula descibing the initial primary excitations and ionizations.[14] The inserted total energy is normalized according to the electronic stopping power. Numerical solution to the equations can then be obtained to describe the spatio-temporal evolution of the temperature in the atomic lattice.

The main limitation of the model is that the value of the electron-phonon coupling constant, g, is not known for insulators. Therefore this value is left as a free parameter which is fitted to track radii.[15] The model also includes other robust approximations, such as adopting the free-electron model for the excited electrons and lacking a distinction between electrons and electron holes.

As such, the (i-TS) model does not describe the transport of atoms. To describe it for the current study, the Classical Molecular Dynamics method is used. This technique can be used to calculate the trajectories of atoms. The forces on the atoms are evaluated from a single parametrized (ground state) electron potential energy function, which is very efficient computationally. However, the excitations in the electronic subsystem and their coupling to the ions are therefore not explicitly taken into account. Rather, the effect of the excitations is included in the energy deposition calculated from the i-TS model.

References

[1] Blender Foundation. Blender open source 3d computer graphics software. URL: `http://www.blender.org`.

[2] Barth C. Atomic Blender Plugin. URL: `http://development.root-1.de/Atomic_Blender_XYZ.php`.

[3] Kluth P, Schnohr CS, Pakarinen OH, Djurabekova F, Sprouster DJ, Giulian R, Ridgway MC, Byrne AP, Trautmann C, Cookson DJ, Nordlund K, Toulemonde M. Fine structure in swift heavy ion tracks in amorphous SiO_2. Phys Rev Lett. 2008;101:175503.

[4] Deal B, Snow E, Mead C. Barrier energies in metal-silicon dioxide-silicon structures. J Phys Chem Solids. 1966;27(11-12):1873 –1879.

[5] Awazu K, Wang X, Fujimaki M, Komatsubara T, Watanabe J, Matsumoto Y, Warisawa S, Ishihara S. The fabrication of aligned pairs of gold nanorods in SiO_2 films by ion irradiation. Nanotechnology. 2009;20:325303.

[6] Leino AA, Pakarinen OH, Djurabekova F, Nordlund K. A study on the elongation of embedded Au nanoclusters in SiO_2 by swift heavy ion irradiation using MD simulations. Nucl Instr Meth Phys Res B. 2012;282:76 –80.

[7] Ulrich S, Nilius N, Freund HJ, Martinez U, Giordano L, Pacchioni G. Realization of an atomic sieve: Silica on Mo(110). Surface Science. 2009;603(8):1145 –1149.

[8] Antonietti JM, Michalski M, Heiz U, Jones H, K.H L, Rösch N, Vitto A, Pacchioni G. Optical Absorption Spectrum of Gold Atoms Deposited on SiO_2 from Cavity Ringdown Spectroscopy. Phys Rev Lett. 2005;94:213402.

[9] Lim KH, Zakharieva O, Shor AM, Rsch N. Modeling metal adsorption at amorphous silica: Gold atoms and dimers as example. Chem Phys Lett. 2007;444(46):280–286.

[10] Ziegler JF, Biersack JP, Littmark U. The Stopping and Range of Ions in Matter. New York: Pergamon; 1985.

[11] Haynes WM. CRC Handbook of Chemistry and Physics, 93rd Edition (Internet Version 2013). Boca Raton, FL, USA: CRC Press/Taylor and Francis; 2012-2013.

[12] Toulemonde M, Assmann W, Dufour C, Meftah A, Studer F, Trautmann C. Experimental phenomena and thermal spike model description of ion tracks in amorphisable inorganic insulators. Mat Fys Medd Kong Dan Vid Selsk. 2006;52:263.

[13] Itoh N, Duffy DM, Khakshouri S, Stoneham AM. Making tracks: electronic excitation roles in forming swift heavy ion tracks. J Phys Condens Matter. 2009;21:474205.

[14] Waligórski RM, Hamm RN, Katz R. The Radial Distribution of Dose around the Path of a Heavy Ion in Liquid Water. Nucl Tracks Meas. 1986;11:309.

[15] Toulemonde M, Costantini JM, Dufour C, Meftah A, Paumier E, Studer F. Track creation in SiO2 and BaFe12O19 by swift heavy ions: a thermal spike description. Nucl Instr Meth Phys Res B. 1996;116(1-4):37 –42.